

# Ethanol dehydration via azeotropic distillation with gasoline fractions as entrainers: A pilot-scale study of the manufacture of an ethanol-hydrocarbon fuel blend.

Vicente Gomis\*, Ricardo Pedraza, María D. Saquete,  
Alicia Font, Jorge García-Cano.

Dpto. Ingeniería Química. Universidad de Alicante. P.O. Box 99 E-03080 Alicante (Spain)

**Keywords:** Ethanol dehydration, azeotropic distillation, hexane, cyclohexane, isooctane, toluene

## Abstract

We establish experimentally and through simulations the economic and technical viability of dehydrating ethanol by means of azeotropic distillation, using a hydrocarbon as entrainer. The purpose of this is to manufacture a ready-to-use ethanol-hydrocarbon fuel blend. In order to demonstrate the feasibility of this proposition, we have tested an azeotropic water-ethanol feed mixture, using a hydrocarbon as entrainer, in a semi pilot-plant scale distillation column. Four different hydrocarbons (hexane, cyclohexane, isooctane, and toluene) that are representative of the hydrocarbons present in ordinary gasoline have been tested. Each of these hydrocarbons was tested separately in experiments under conditions of constant feed rate and variable reboiler heat duty. The experimentally obtained results are compared with results calculated by a simulator. Finally, the proposed and traditional ethanol dehydration processes are compared to ascertain the advantages of the former over the latter.

## 1. Introduction

The fermentation of biomass represents a promising means of obtaining biofuels – one that involves lower emissions of polluting gases into the atmosphere. Bioethanol is one of the most widely used of these biofuels, and the manufacture thereof from raw materials requires several rounds of treatment, including milling, fermentation and distillation, before a water-ethanol azeotrope can be obtained. A dehydration step usually follows at this point, for which there are many different available techniques [1, 2], such as adsorption on molecular sieves [3], azeotropic distillation [4], pressure swing distillation [5], pervaporation [6], extractive distillation with ionic liquids [7], etc.

Traditional methods of bioethanol manufacture involve producing pure ethanol for subsequent addition to a fuel blend. In the past, azeotropic distillation was the most commonly used method to obtain pure ethanol using benzene [8], ciclohexane [9], hexane [10], toluene [11], isooctane [12]... as entrainers. Currently the bioethanol is generally dehydrated by the biofuel manufacturer by means of molecular sieves, and then kept in storage for later addition to gasoline in legally mandated proportions. At present, European legislation mandates 10% [13] as the maximum permitted gasoline ethanol-content, and 0.3% [14] as the maximum permitted bioethanol water-content.

However, the novel process that we present in this paper would lead to the manufacture of an ethanol-hydrocarbon blend that is immediately ready for use as fuel, with gasoline itself serving as the separating agent. In practice, this blend would be manufactured at refineries via azeotropic distillation,

---

\* Corresponding author. Tel + 34 965903867. E-mail: vgomis@ua.es

46 and then distributed directly to gas stations.

47 Gasoline is a complex mixture of hydrocarbons and our intention here is to embark on a systematic  
48 study of the process that is the subject of this paper. So, as the first step in a more ambitious research  
49 effort, we have selected a series of hydrocarbons we consider to be representative of the different  
50 hydrocarbon fractions present in gasoline. Thus, to represent the straight-chain hydrocarbon fractions  
51 in gasoline, we chose hexane; to represent cyclic hydrocarbons, we chose cyclohexane; isooctane for  
52 branched hydrocarbons; finally, toluene served to represent the aromatic fractions. Each of these was  
53 tested in an azeotropic distillation column at the semi pilot-plant scale, in order to gauge the technical  
54 feasibility of a process that obtains such a ready-to-use fuel blend. To establish whether the  
55 hydrocarbons are suitable for use in this process under different operating conditions, as well as for  
56 purposes of comparison with the conventional process, we have simulated the experiments using  
57 equilibrium data.

58 Ultimately, our intention is to show that it is both technically and economically feasible to obtain, via  
59 azeotropic distillation, a bioethanol-hydrocarbon fuel blend that is immediately ready for use in  
60 modern motor vehicles. Additionally, the new process would represent an improvement over current  
61 best practice.

62

## 63 **2. Materials and methods**

### 64 2.1 Chemicals

65

66 The chemical purity grades of the tested hydrocarbons were as follows: hexane (min 98.5%),  
67 cyclohexane (min 99.5%), isooctane (min 99%) and toluene (min 99%); all were purchased from the  
68 commercial supplier PANREAC. Analytical grade ethanol and 2-propanol, supplied by MERCK, were  
69 used to prepare the standards (min 99.9 and 99.8%, respectively). The deionized water that was used  
70 had a measured conductivity of 3  $\mu\text{S}/\text{cm}$ .

71

### 72 2.2 Equipment

73

74 A 50mm diameter Armfield UOP3CC column, fitted with eight plates and built to the scale of a semi  
75 pilot plant was used. Details of the equipment can be found in a prior publication [15]. Only one minor  
76 modification was made to it for the purpose of the present study: the column and the boiling chamber  
77 were wrapped with thermal insulation. The insulating material was Armaflex AF (Armacell Advanced  
78 Insulation), supplied by PecoMark. Figure 1 shows a schematic diagram of the experimental setup.  
79 The label C stands for column, D is for decanter, HE denotes various heat exchangers and TM refers  
80 to the many points where sampling took place.

81

82 Based on the capacity and characteristics of the column, as well as our objective of obtaining a 5%  
83 w/w ethanol concentration in the bottoms product, below the legal limit, the flow rate of the various  
84 hydrocarbon entrainers was fixed at 41 g/min, while the water-ethanol mixture's was 4.38 g/min. The  
85 composition of the latter was approximately 93% w/w ethanol and 7% w/w water, which is close to  
86 composition of the binary azeotrope. The temperature of the various streams and process units varied  
87 depending on the hydrocarbon, and took into account its boiling point temperature. Table 1 lists those  
88 temperatures:

89

### 90 2.3 Sampling and analysis

91

92 The compositions of the samples were determined by chromatography with 2-propanol as internal  
93 standard at a standard deviation of 2%. The composition of the water was compared with that obtained

94 by Karl-Fischer titration at a standard deviation of 1%. A detailed description of the sampling  
95 and analytical methods used to determine the concentrations of the column exit streams can be  
96 found elsewhere[15].

97

### 98 **3. Experimental Results**

99 Multiple experiments were carried out on each of the hydrocarbons. There are many variables that can  
100 affect the distillation process: the mass ratio between ethanol and entrainer, the reboiler heat duty, the  
101 entrainer compound, flow rates, temperatures, etc. Only two of these variables were chosen for  
102 studying the process, the entrainer and heat duty, while the rest were kept constant. Notice that the  
103 purpose of this study was to ascertain the feasibility of the proposed process as well as to identify  
104 problems that might arise in the industrial implementation thereof.

105 Once steady state had been reached (after at least an hour), which was ascertained by repeatedly  
106 measuring the water content in the bottoms stream, we also measured flow rates and determined the  
107 compositions of all streams. With this information, it is possible to verify whether the conditions of  
108 material balance had been satisfied at all the sampling points. Of all the concentrations tested, the  
109 bottoms stream water-content was given particular attention since excess water in the fuel blend would  
110 mean it no longer met legal requirements.

111

112 Figures 2 to 5 show three graphs of several results obtained for each tested hydrocarbon, plotted as a  
113 function of reboiler heat duty. Each Figure contains a plot of the flow rates of the top and bottoms  
114 streams of the column (Figures 2-5 a), the ethanol and hydrocarbon concentrations in the bottoms  
115 (Figures 2-5 b) and finally, the water concentration in the bottoms (Figures 2-5c). It is the latter  
116 quantity that permits assessing the feasibility of the process.

117

118

119 It was found in all cases that there was a maximum value of the reboiler heat duty beyond which the  
120 column no longer operated correctly. This was evident from the fact that the vapor leaving the top of  
121 the column did not split into two liquid phases on cooling. However, we must emphasize that neither  
122 this maximum nor any of the other reboiler heat duties can be compared across different mixtures  
123 since they depend on other operating variables such as the temperature of the hydrocarbon in the  
124 column feed; this differs from hydrocarbon to hydrocarbon simply because they have different boiling  
125 point temperatures, as shown in Table 1.

126

127 Figures 2-5 a show that the distillate flow rates are small compared with the overall feed rate (about 45  
128 g/min). They remain essentially constant or increase slightly with the exception of the system  
129 containing cyclohexane, whose flow rate increases markedly.

130

131 As regards the bottoms stream flow rates (Figures 2-5 a), they are roughly the same as the feed flow  
132 rate (45 g/min), and as in the case of the distillate, also remain essentially constant with the exception  
133 of the mixture containing cyclohexane (Figure 3 a), which experiences a marked decrease in flow rate  
134 as the reboiler heat duty increases.

135

136 The mass fraction of water in the waste stream (Figures 2-5 c) is the key parameter here since it will  
137 allow us to determine whether it is actually feasible to produce a fuel blend by ethanol dehydration  
138 using the method presented in this paper. In this regard, we observe the same behavior of all the  
139 mixtures we tested: on increasing the reboiler heat duty, the mass fraction of water in the waste stream  
140 decreases sharply. This is how we achieved our objective of obtaining an ethanol-hydrocarbon product  
141 that is nearly water-free: by increasing the reboiler heat duty. After the period of rapid decrease in the  
142 mass fraction of water, which remained very low subsequently, we observed only small fluctuations in  
143 its value. In any event, the obtained values did not exceed the maximum legal limit of 0.00015 (%  
144 w/w), which is equivalent to a maximum of 0.3% ethanol water-content in a blend containing 5%  
145 ethanol[14].

146

147 On the other hand, the mixture containing cyclohexane (Figure 3) behaved rather differently. The  
148 observed fluctuations in flow rates and compositions of this mixture are significantly larger than in the  
149 case of the other mixtures. This likely has to do with the small differences in shape of the solubility  
150 curve between this mixture and the others in the working range of the distillation column. This  
151 working range is close to the mixture's plait point, and there usually is not much experimental liquid-  
152 liquid equilibrium data available in this range to permit a detailed study. Such data are not easy to  
153 determine since small changes in the composition of the global mixture lead to large ones in the  
154 composition of the equilibrium liquid phases.

155 In conclusion, it is important to point out that all the studied hydrocarbons are suitable for producing  
156 an ethanol-hydrocarbon mixture that is nearly free of water. Consequently, it is not unreasonable to  
157 expect this to apply also to a mixture of several hydrocarbons, which would permit the eventual use of  
158 gasoline as entrainer in the manufacture of a ready to use ethanol-hydrocarbon fuel blend.

159

#### 160 **4. Simulation**

161

162 For a proper design of the ethanol dehydration process considered here, commercial simulation  
163 software packages must possess a series of equations and parameters that will enable calculation of  
164 both the vapor-liquid equilibrium in the distillation column as well as the liquid-liquid and vapor-  
165 liquid-liquid equilibria in the decanter. In general, thermodynamic models tend to reproduce these  
166 equilibria more or less correctly. However, as was pointed out in another study [16], near the plait

167 point in the heterogeneous region of the mixture there always arises a systematic discrepancy between  
168 experimental and thermodynamically modeled data. The models generally produce a heterogeneous  
169 region for water-ethanol-hydrocarbon mixtures that is larger than is observed experimentally, and  
170 especially near the plait point, which happens to overlap with the working range of the decanter, as  
171 mentioned earlier. Furthermore, these models are known to fail to reproduce the marked asymmetry  
172 observed in the non-isothermal binodal curves of the above mixtures. As a general rule, the  
173 heterogeneous regions calculated from correlation parameters are always larger and shifted more  
174 toward the ethanol-hydrocarbon binary than is observed experimentally [17, 18, 19, 20].

175

176 The consequence is that errors arise when trying to simulate the proposed process by means of  
177 commercial software employing conventional thermodynamic models to determine the liquid-liquid  
178 equilibrium. The most glaring error is a failure to predict a maximum reboiler heat duty at which point  
179 the process ceases to run correctly, when experimentally this is exactly what is observed because two  
180 phases no longer appear in the decanter. This error arises because the size of the heterogeneous region  
181 calculated by the model is larger than is found experimentally, and is, as was pointed out earlier,  
182 exactly what thermodynamic models would predict for water-ethanol-hydrocarbon mixtures.

183

184 The various experiments conducted on each of the hydrocarbon mixtures in the azeotropic distillation  
185 column have been simulated by means of the commercially available software Chemcad 6 [21]. The  
186 operating variables were assigned the same values as in the laboratory experiments. The UNIFAC  
187 model was used to determine the vapor-liquid equilibrium data because the equilibrium data calculated  
188 in this way have been found to compare favorably with experiment. However, it was necessary to  
189 design a special process unit to calculate the separation of the liquid phases in the decanter. In an  
190 attempt to avoid the discrepancies encountered in correlations using conventional models, the liquid-  
191 liquid equilibrium data were instead calculated by means of interpolation of experimental data from  
192 the literature. This was accomplished by making simultaneous use of two equations: on the one hand,  
193 a “spline” interpolation [22] was used, which is a set of cubic interpolations through a minimum of  
194 five points, to fix the position of the binodal curve; on the other, the ratio between the equilibrium  
195 aqueous and organic phases was determined via Hand’s equation [23].

196

197 Figure 6 shows the simulation scheme, and includes the following process units:

198

199 Unit 1 (C): Distillation column. The column used in the experiments was fitted with 8 plates and a  
200 reboiler. The efficiency of the distillation stages in simulations has been estimated to be 0.6-0.7  
201 following the criterion by Stichlmair y Fair 1998 [24]. Therefore, based on this, we selected a column  
202 with 6 equilibrium stages. The column does not use a condenser, whose function is instead carried out  
203 by unit 2 in Figure 6.

204

205 Unit 2 (HE-1): Heat exchanger. This unit controls the temperature of vapor stream 8, which leaves  
206 from the top of the column. This temperature is set to the temperature at which decanting of phases  
207 takes place in the experiments.

208

209 Unit 3 (U-1): This unit determines whether stream 9 contains one or two liquid phases. If the  
210 composition of stream 9 is in the homogeneous region (according to the curve obtained by the “spline”  
211 interpolation), it is recycled back to the column. If it falls in the heterogeneous region, on the other  
212 hand, the stream passes on to unit 4.

213

214 Unit 4 (U-2): This process unit carries out the separation of phases by taking into account both the  
215 spline interpolation and the correlation via Hand’s equation. The phase of largest hydrocarbon mass

216 fraction leaves in stream 4 and is recycled back to the column, while the one containing the most water  
217 leaves in stream 5.

218

219 Unit 5 (M): This combines streams 4 and 11. Note that unit 5 receives either one or both of these  
220 streams, which is determined by unit 3.

221

222 Unit 6 (HE-2): This heat exchanger raises the temperature of the recycle stream to the experimental  
223 working temperature.

224

225 Based on the flow diagram in Figure 6 and by varying only the supplied reboiler heat duty, we have  
226 simulated the experiments. The results are plotted in Figures 2 to 5, which also show the experimental  
227 results. Since heat losses to the surroundings are not accounted for in the simulations, the simulation  
228 reboiler heat duty values are shifted with respect to the experimental values on the horizontal axes.

229

230 First of all, it is worth mentioning that the above method of calculating the liquid-liquid equilibrium  
231 produces a maximum reboiler heat duty beyond which azeotropic distillation is no longer possible.  
232 This result is not obtained when models such as NRTL, UNIQUAC or UNIFAC are used to determine  
233 the liquid-liquid equilibrium, and is a consequence of the prediction by these models, with rising  
234 reboiler heat duty, of a composition of the vapor leaving the top of the column that lies in the  
235 heterogeneous region, when in reality it should lie in the homogeneous region.

236

237 On comparing the simulation and experimental results, we observe that very similar bottoms and top  
238 product flow rates are obtained, respectively. The greatest deviation from this trend occurs in the case  
239 of the mixture containing cyclohexane, whose experimental distillate flow rate increases markedly  
240 with reboiler heat duty. At the same time, its bottoms product flow rate falls. The simulation results  
241 exhibit the same trend, but not the pronounced fluctuations observed in the experiment. This could be  
242 due to the small differences between the experimental and simulation solubility curves.

243

244 As regards the bottoms product (the ethanol-hydrocarbon blend destined for use as fuel), the  
245 proportions of ethanol and hydrocarbon in the simulations and experiments are similar. The water  
246 content of the bottoms also exhibits the same trend in simulation and experiment.

247

## 248 **5. Comparison with the conventional process**

249 Now that it has been established that the experimental and simulated results agree reasonably well and  
250 that simulations are capable of reproducing the desired bottoms product, we proceed to compare the  
251 conventional process of ethanol manufacture with the one described in this study. The conventional  
252 process to obtain pure ethanol, with benzene as entrainer, is discussed extensively in the literature  
253 [25].

254 For the purpose of the comparison, the simulation has been based on a flow diagram similar to the one  
255 shown in Figure 7. UNIFAC was used to model the thermodynamics of all process units.

256 Table 2 lists the temperatures, flow rates and compositions of the feed and product streams of the two  
257 processes that were studied with isooctane as separating agent. Streams 1 and 2 represent the water-  
258 ethanol azeotrope and hydrocarbon feed streams, respectively; they are the same in both processes.  
259 Stream 3 represents the desired product, which in the conventional process is pure ethanol, and in the  
260 proposed process is the ethanol-hydrocarbon blend. The water that has entered the system leaves it in  
261 stream WS, and corresponds to the bottoms product from the second distillation column whose  
262 function is also to remove water from the system.

263

264 If we compare the heat requirements of the process units in the two simulated processes (see Table 3)  
265 and the energy to produce anhydrous ethanol in each case (see Table 4), we obtain a threefold  
266 reduction in costs of the new process with respect to the conventional one. This leads us to believe that  
267 the new process would be a viable alternative to the conventional process.

268

## 269 **6. Conclusions**

270 We have shown experimentally and by simulation that it is viable both technically and economically  
271 to manufacture a ready-to-use ethanol-hydrocarbon fuel blend by azeotropic distillation.

272 Starting from an azeotropic mixture of water and ethanol, and with several different hydrocarbons  
273 acting as entrainers (hexane, cyclohexane, isooctane and toluene), we have demonstrated the technical  
274 viability of this process in a distillation column at the semi pilot-scale. This is based on the fact that  
275 the ethanol-hydrocarbon fuel blend obtained as final product contains less water than is stipulated by  
276 the EU legislation currently in force.

277 The various experiments carried out in this study show that, at a given feed rate, as the reboiler heat  
278 duty rises, the amount of water in the ethanol-hydrocarbon blend falls until the heat duty reaches a  
279 maximum value at which the distillation column ceases to operate correctly.

280

281 Conventional thermodynamic models exhibit departures from observed behavior when used to  
282 correlate experimental data, and particularly in the case of liquid-liquid equilibria in the vicinity of the  
283 plait point, which also happens to be in the vicinity of the operating range of the column. To avoid  
284 such departures, other methods of interpolating equilibrium data are required, as otherwise we would  
285 not find maximum reboiler heat duty values that result in distillation column malfunction. A  
286 simulation of the process in Chemcad with the above considerations taken into account produces  
287 results that agree well with experiment.

288

289 The simulation results of the proposed process indicate that there is a threefold reduction in heat duties  
290 compared to heteroazeotropic distillation, which produces pure ethanol.

291

- 293 (1) Vane L.M. Separation technologies for the recovery and dehydration of alcohols from fermentation  
294 broths. *Biofuels, Bioprod. Bioref.* **2008**, 2, 553–588
- 295 (2) Frolkova, A.K.; Raeva, V.M. Bioethanol Dehydration. *Theor. Found. of Chem. Eng.* **2010**, 44 (4)  
296 545-556
- 297 (3) Weitkamp, J.; Ernst, S. Separation of gaseous water/ethanol mixtures by adsorption on  
298 hydrophobic zeolites. *Zeolites* **1991**, 11( 4), 314-317
- 299 (4) Widadgo, S.; Seider, W.D. Azeotropic distillation. *AIChE J.* **1996**, 42(1), 96-130
- 300 (5) Knapp, J.P.; Doherty, M.F. A New PressureSwing-Distillation Process for Separating  
301 Homogeneous Azeotropic Mixtures. *Ind. Eng. Chem. Res.* **1992**, 31, 346-357
- 302 (6) Le, N.L.; Wang, Y. and Chung,T. Synthesis, cross-linking modifications of 6FDA-NDA/DABA  
303 polyimide membranes for ethanol dehydration via pervaporation. *J. Membr. Sci.* **2012**, 415-416, 109-  
304 121
- 305 (7) Pereiro, A.B.; Araujo, J.M.M.; Esperança, J.M.S.S.; Marrucho, I.M.; Rebelo, L.P.N. Ionic liquids  
306 in separations of azeotropic systems-a review. *J. Chem. Thermodynamics.* **2012**, 46, 2-28
- 307 (8) Young, S. The preparation of absolute alcohol from strong spirit. *J. Chem. Soc. Trans.* **1902**, 81,  
308 707-717
- 309 (9) Kirk-Othmer *Encyclopedia of Chemical Technology*, 4th Edition, New York: Wiley; **1993** Vol.8
- 310 (10) Stratula, C.; Oprea, F.; Mihaescu, D. Separation and purification of anhydrous ethanol by  
311 azeotropic distillation using an entrainer. *Revista de Chimie* , **2005**, 56 (5), 544-548
- 312 (11) Perry's Chemical Engineers Handbook 7<sup>th</sup> Edition, MacGraw-Hill **2001**, Vol.2
- 313 (12) Font ,A.; Asensi, J. C., Ruiz F.; Gomis V. Application of Isooctane to the Dehydration of Ethanol.  
314 Design of a Column Sequence To Obtain Absolute Ethanol by Heterogeneous Azeotropic Distillation  
315 *Ind. Eng. Chem. Res.* **2003**,42, 140-144
- 316 (13) Directive 2009/30/EC of the European Parliament and of the council of 23 April **2009**
- 317 (14) EN 15376. Automotive fuels - Ethanol as a blending component of petrol - Requirements and test  
318 methods, **2011**.
- 319 (15) Gomis, V.; Pedraza, R.; Francés, O.; Font, A.; Asensi, J. C. Dehydration of Ethanol Using  
320 Azeotropic Distillation with Isooctane. *Ind. Eng. Chem. Res.* **2007**, 46, 4572-4576.
- 321 (16) Lee, B. H.; Qin, Y.; Prausnitz, J.M. Thermodynamic representation of ternary liquid–liquid  
322 equilibria near-to and far-from the plait point. *Fluid Phase Equilib.* **2006**, 240, 67–72.
- 323 (17) Font, A.; Asensi, J. C.; Ruiz, F.; Gomis, V. Application of Isooctane to the Dehydration of  
324 Ethanol. Design of a Column Sequence To Obtain Absolute Ethanol by Heterogeneous Azeotropic  
325 Distillation. *Ind. Eng. Chem. Res.* **2003**, 42, 140-144.
- 326 (18) Gomis, V.; Font, A.; Pedraza, R.; Saquete, M.D. Isobaric vapor–liquid and vapor–liquid–liquid  
327 equilibrium data for the system water + ethanol + cyclohexane. *Fluid Phase Equilib.* **2005**, 235, 7–10.
- 328 (19) Gomis, V.; Font, A.; Pedraza, R.; Saquete, M.D. Isobaric vapor–liquid and vapor–liquid–liquid  
329 equilibrium data for the water–ethanol–hexane system. *Fluid Phase Equilib.* **2007**, 259, 66–70.
- 330 (20) Gomis, V.; Font, A.; Saquete, M.D. Homogeneity of the water + ethanol + toluene azeotrope at  
331 101.3 kPa. *Fluid Phase Equilib.* **2008**, 266, 8–13.
- 332 (21) Chemcad 6. Process Flow sheet Simulator, Chemstations Inc.: Houston, **2008**
- 333 (22) Akima, H. A New Method of Interpolation and Smooth Curve Fitting Based on Local Procedures.  
334 *Journal of the association for computing machinery* **1970**, 17, 589-602.
- 335 (23) Treybal, R.E. *Extracción en fase líquida*; Unión tipográfica editorial hispano americana: Mexico,  
336 **1968**.
- 337 (24) Stichlmair, J. G.; Fair, J. R. *Distillation: Principles and Practice*; Wiley-VCH: New York, **1998**.
- 338 (25) Doherty, M. F.; *Conceptual design of distillation systems*, McGraw-Hill: Boston, **2001**
- 339



340 **Tables**

341

342 **Table 1:** Temperatures of the streams and process units for the various studied mixtures.

	Temperature (K)			
Hydrocarbon	Water-ethanol feed	Hydrocarbon feed	Decanter	Reflux
Hexane	323	331	305	329
Cyclohexane	335	339	309	338
Isooctane	347	367	318	367
Toluene	344	349	298	348

343

344

345 **Table 2:** Temperatures, flow rates and compositions of the feed and product streams for the studied  
346 processes.

<b>Conventional Process</b>				
<b>Stream</b>	<b>1</b>	<b>2</b>	<b>3</b>	<b>WS</b>
Temperature (K)	352.8	367.2	351.1	372.7
Flow rate (g/min)	4.38	$6 \cdot 10^{-5}$	4.13	0.25
Water	0.060	0.000	0.003	0.999
Ethanol	0.940	0.000	0.997	0.001
Isooctane	0.000	1.000	0.000	0.000
<b>Proposed process</b>				
<b>Stream</b>	<b>1</b>	<b>2</b>	<b>3</b>	<b>WS</b>
Temperature (K)	352.8	367.2	346.4	372.7
Flow rate (g/min)	4.38	39.73	43.81	0.26
Water	0.060	0.000	0.000	0.999
Ethanol	0.940	0.000	0.094	0.001
Isooctane	0.000	1.000	0.906	0.000

347

348

349 **Table 3:** Comparison of the energy needs of the simulated process units

<b>Process unit</b>	<b>Column 1 (W)</b>	<b>Condenser (W)</b>	<b>Column 2(W)</b>
Conv Process	275.15	-986.04	711.48
New Process	81.42	-370.64	256.85

350

351

352

353

354 **Table 4:** Comparison of heat duties in the production of anhydrous ethanol

<b>Process unit</b>	<b>Column 1 (W/gEtOH)</b>	<b>Condenser (W/gEtOH)</b>	<b>Column 2 (W/gEtOH)</b>
Conv Process	66.82	-239.47	172.79
New Process	19.83	-90.29	62.57

355

356

357

358 **Figure Captions**

359

360 **Figure 1:** Schematic representation of the equipment used

361

362 **Figure 2 a):** Mixture containing hexane. Plot of several variables against reboiler heat duty:  
363 Experimental and simulated top and bottoms product flow rates

364

365 **Figure 2 b):** Mixture containing hexane. Plot of several variables against reboiler heat duty:  
366 Experimental and simulated composition (% w/w) of ethanol and hexane in the column  
367 bottoms

368

369 **Figure 2 c):** Mixture containing hexane. Plot of several variables against reboiler heat duty:  
370 Experimental and simulated composition (% w/w) of water in the bottoms product.

371

372 **Figure 3 a):** Mixture containing cyclohexane. Plot of several variables against reboiler heat  
373 duty: Experimental and simulated top and bottoms product flow rates

374

375 **Figure 3 b):** Mixture containing cyclohexane. Plot of several variables against reboiler heat  
376 duty: Experimental and simulated composition (% w/w) of ethanol and cyclohexane in the  
377 column bottoms.

378

379 **Figure 3 c):** Mixture containing cyclohexane. Plot of several variables against reboiler heat  
380 duty: Experimental and simulated composition (% w/w) of water in the bottoms product

381

382 **Figure 4 a):** Mixture containing isooctane. Plot of several variables against reboiler heat  
383 duty: Experimental and simulated top and bottoms product flow rates

384

385 **Figure 4 b):** Mixture containing isooctane. Plot of several variables against reboiler heat  
386 duty: Experimental and simulated composition (% w/w) of ethanol and isooctane in the  
387 column bottoms

388

389 **Figure 4 c):** Mixture containing isooctane. Plot of several variables against reboiler heat  
390 duty: Experimental and simulated composition (% w/w) of water in the bottoms product.

391

392 **Figure 5 a):** Mixture containing toluene. Plot of several variables against reboiler heat duty:  
393 Experimental and simulated top and bottoms product flow rates

394

395 **Figure 5 b):** Mixture containing toluene. Plot of several variables against reboiler heat duty:  
396 Experimental and simulated composition (% w/w) of ethanol and toluene in the column  
397 bottoms

398

399 **Figure 5 c):** Mixture containing toluene. Plot of several variables against reboiler heat duty:  
400 Experimental and simulated composition (% w/w) of water in the bottoms product.

401

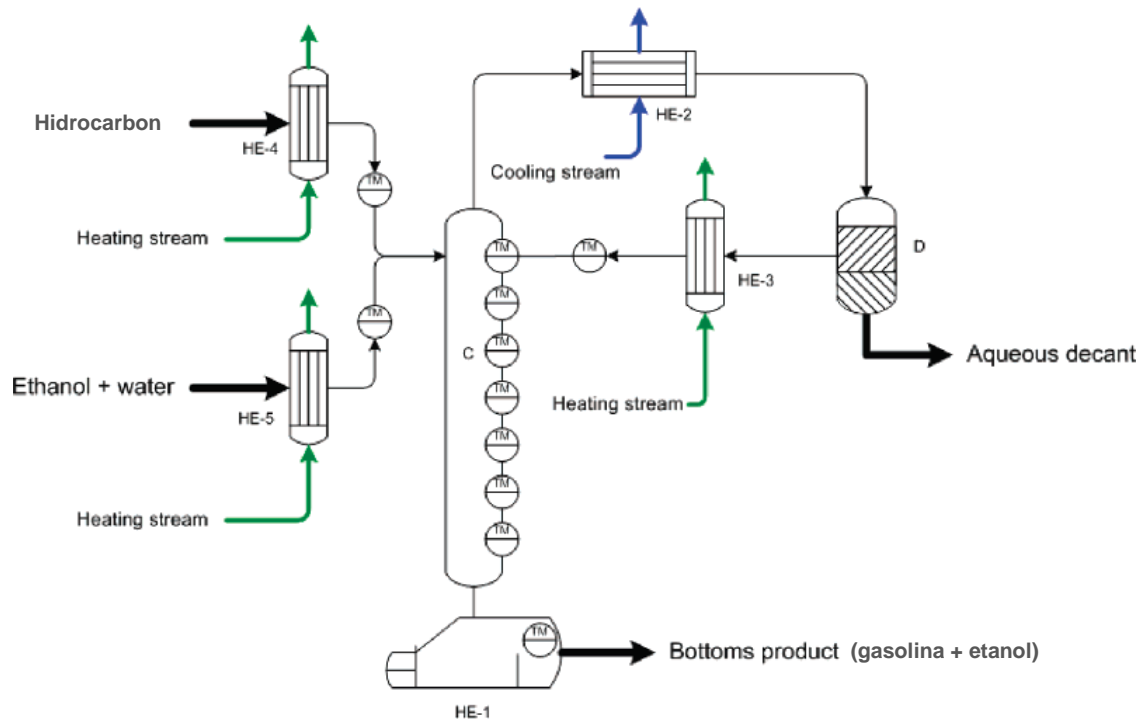
402 **Figure 6:** Schematic diagram for the Chemcad simulation.

403

404 **Figure 7:** Schematic diagram used to compare both processes.

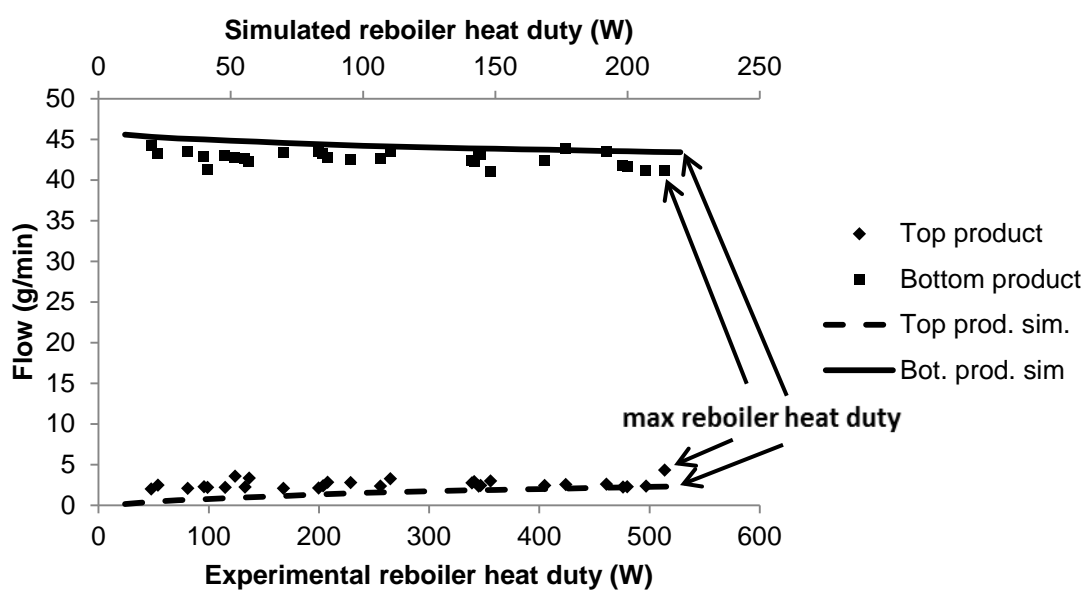
405

406

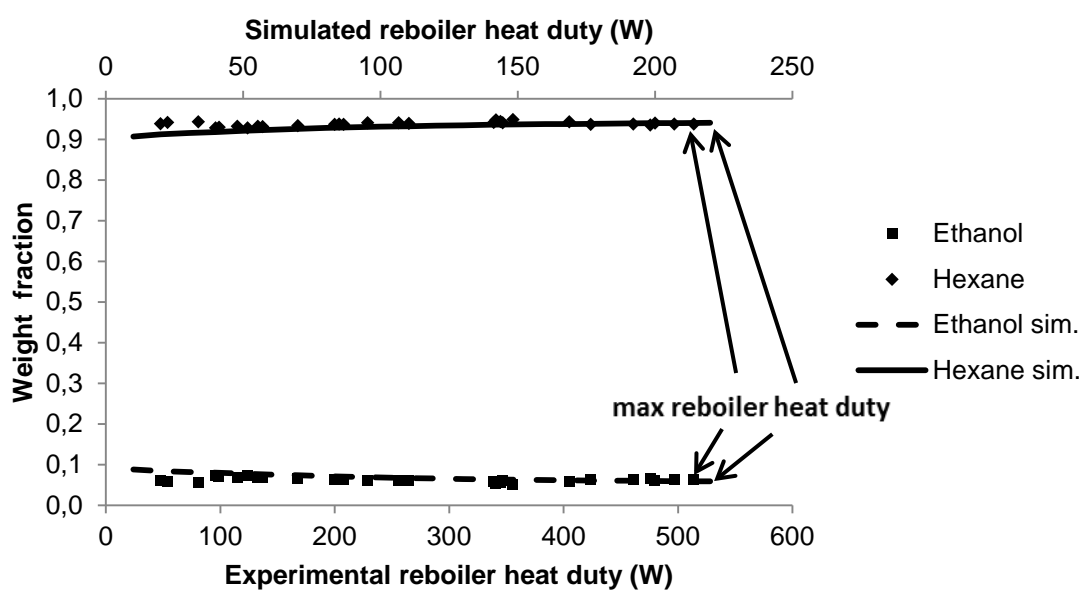


407  
 408  
 409

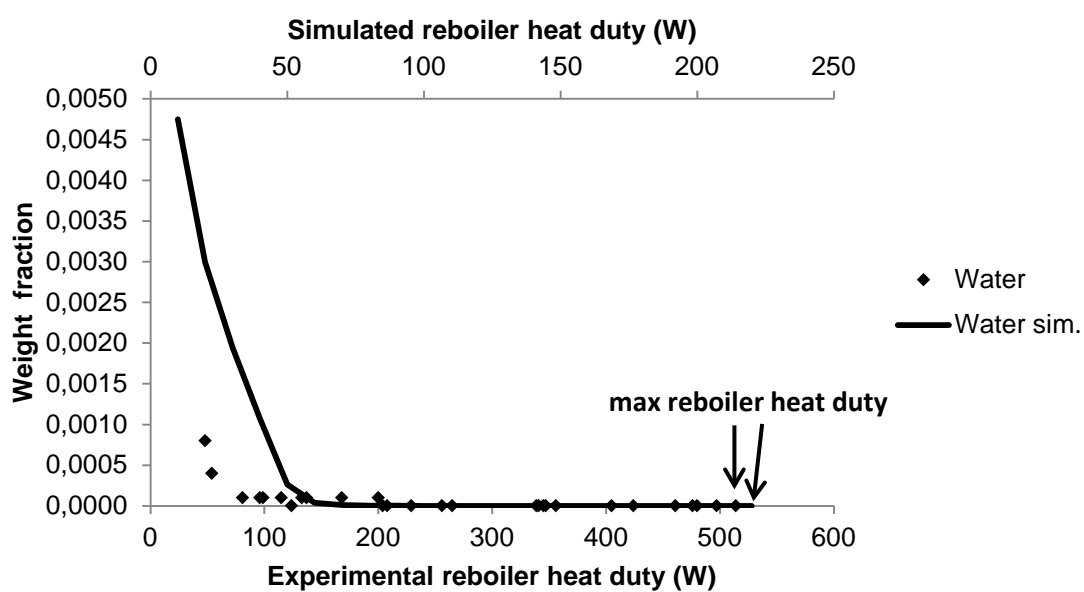
**Figure 1:** Schematic representation of the equipment used



410  
 411 **Figure 2 a):** Mixture containing hexane. Plot of several variables against reboiler heat duty:  
 412 Experimental and simulated top and bottoms product flow rates  
 413

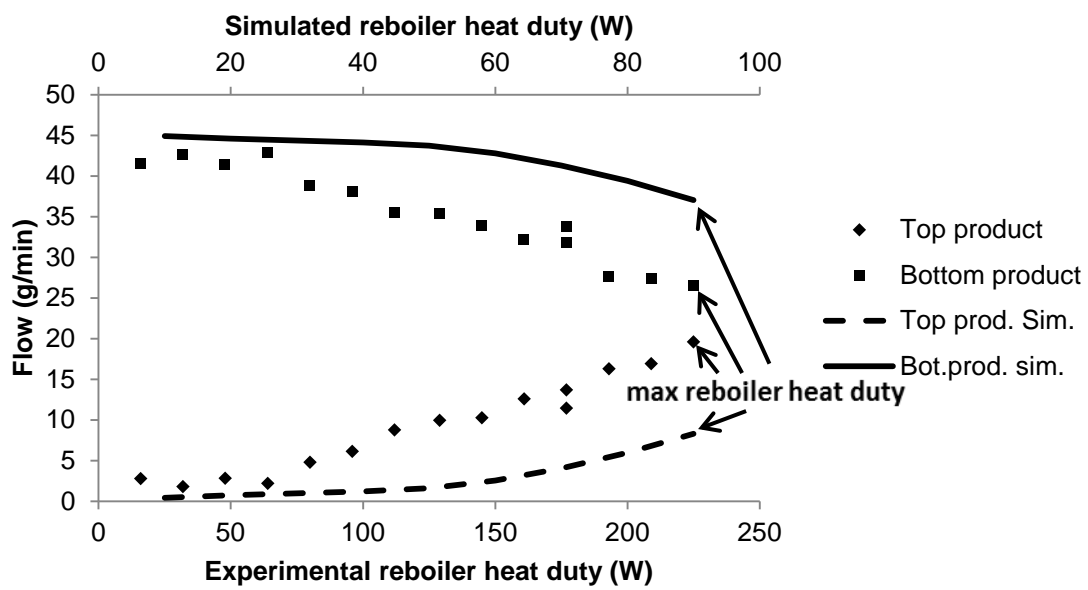


414  
 415 **Figure 2 b):** Mixture containing hexane. Plot of several variables against reboiler heat duty:  
 416 Experimental and simulated composition (% w/w) of ethanol and hexane in the column  
 417 bottoms  
 418

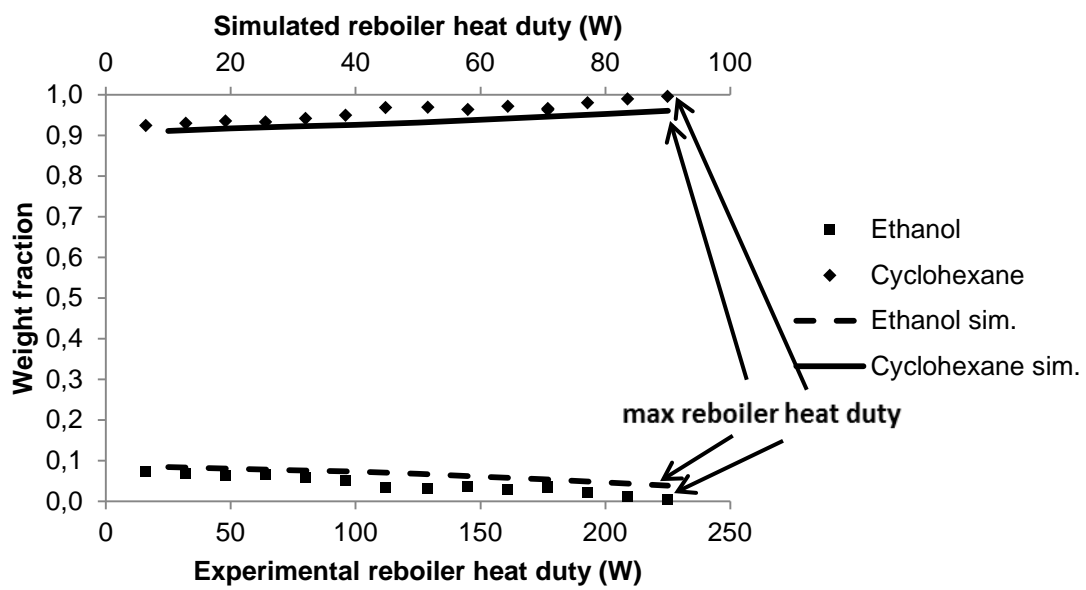


419  
 420 **Figure 2 c):** Mixture containing hexane. Plot of several variables against reboiler heat duty:  
 421 Experimental and simulated composition (% w/w) of water in the bottoms product.  
 422

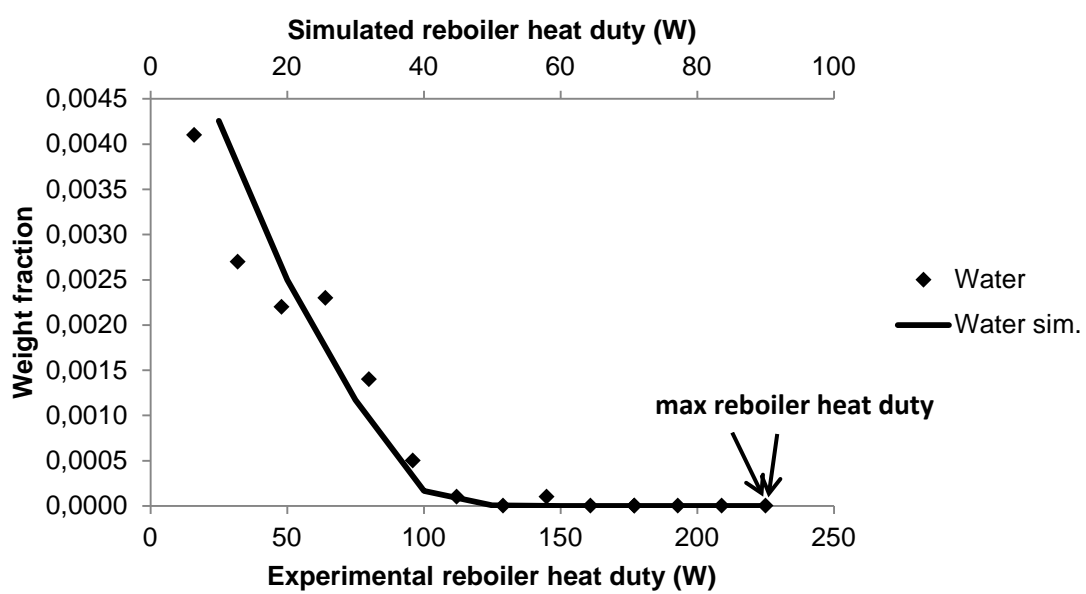




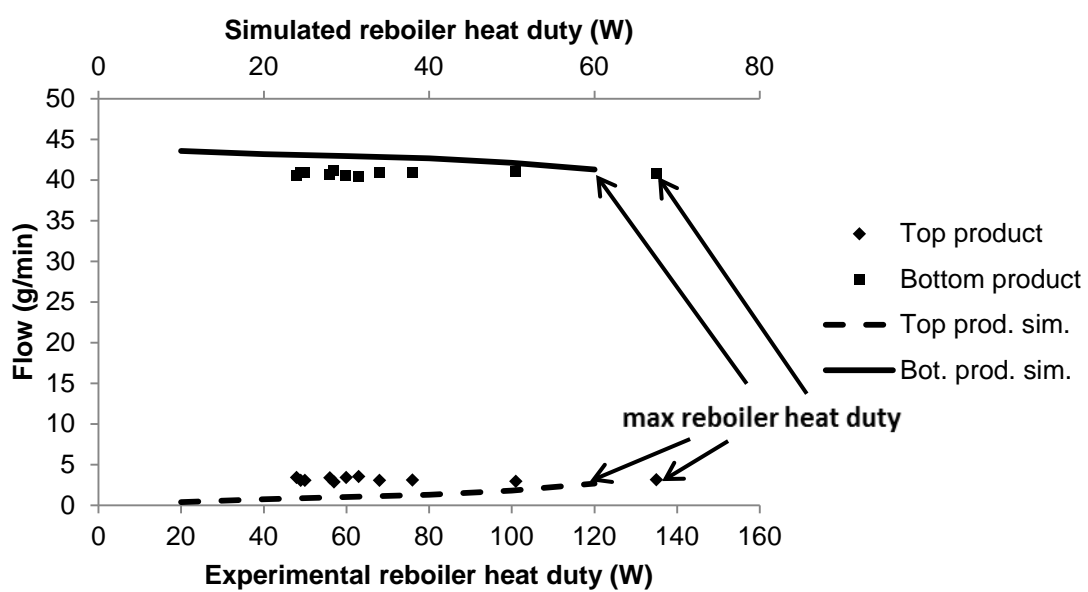
423  
 424 **Figure 3 a):** Mixture containing cyclohexane. Plot of several variables against reboiler heat  
 425 duty: Experimental and simulated top and bottoms product flow rates  
 426



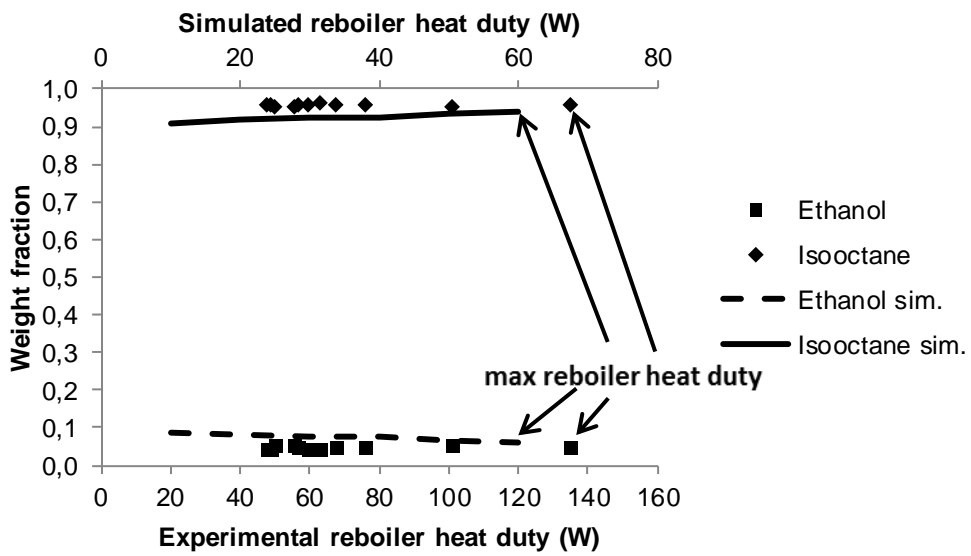
427  
 428 **Figure 3 b):** Mixture containing cyclohexane. Plot of several variables against reboiler heat  
 429 duty: Experimental and simulated composition (% w/w) of ethanol and cyclohexane in the  
 430 column bottoms.  
 431



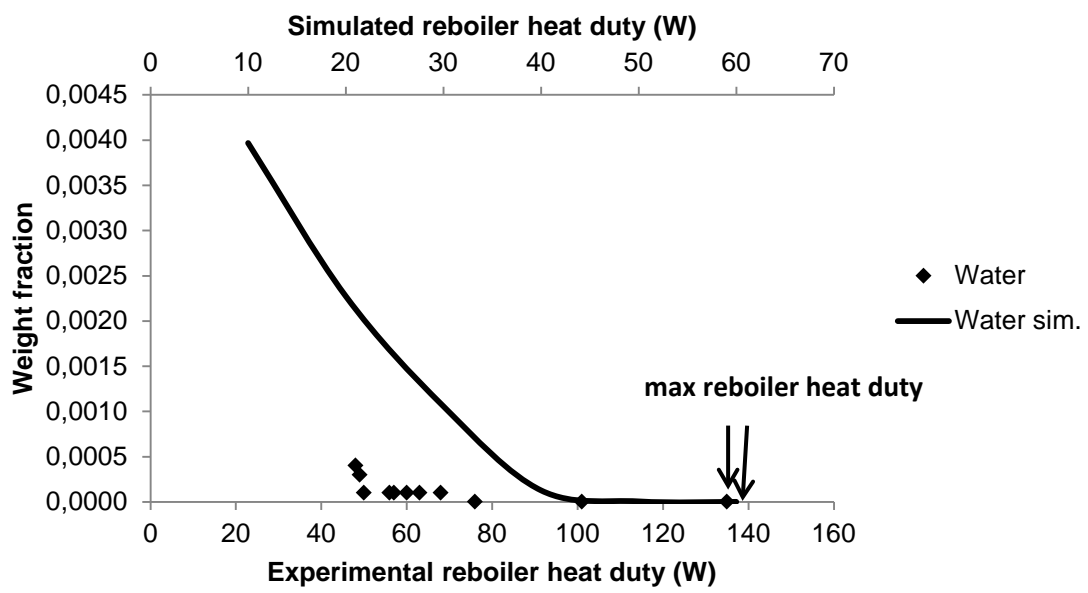
432  
 433 **Figure 3 c):** Mixture containing cyclohexane. Plot of several variables against reboiler heat  
 434 duty: Experimental and simulated composition (% w/w) of water in the bottoms product.  
 435  
 436



437  
 438 **Figure 4 a):** Mixture containing isooctane. Plot of several variables against reboiler heat duty:  
 439 Experimental and simulated top and bottoms product flow rates  
 440

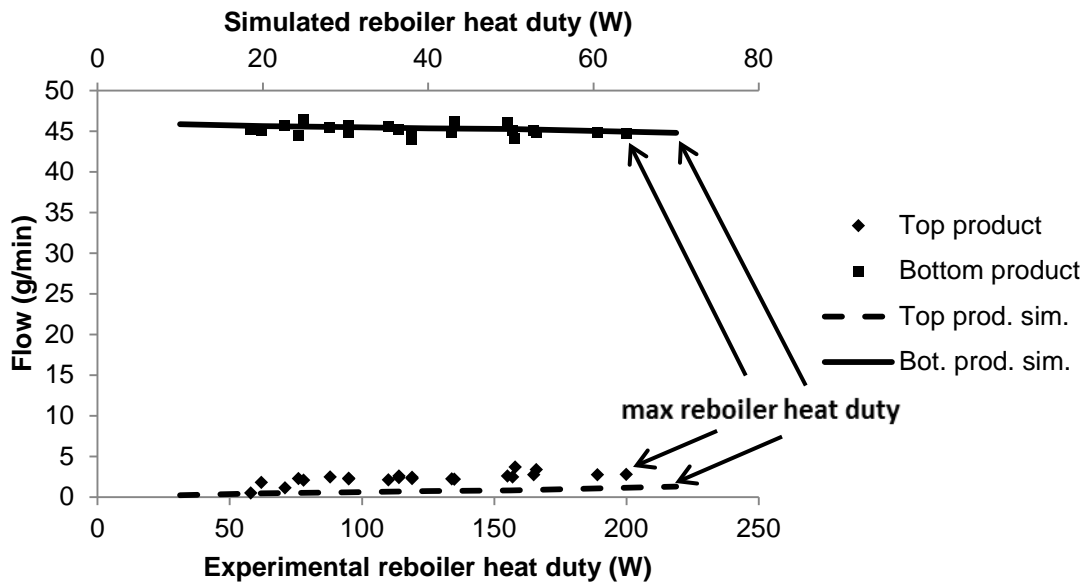


441  
 442 **Figure 4 b):** Mixture containing isooctane. Plot of several variables against reboiler heat  
 443 duty: Experimental and simulated composition (% w/w) of ethanol and isooctane in the  
 444 column bottoms  
 445



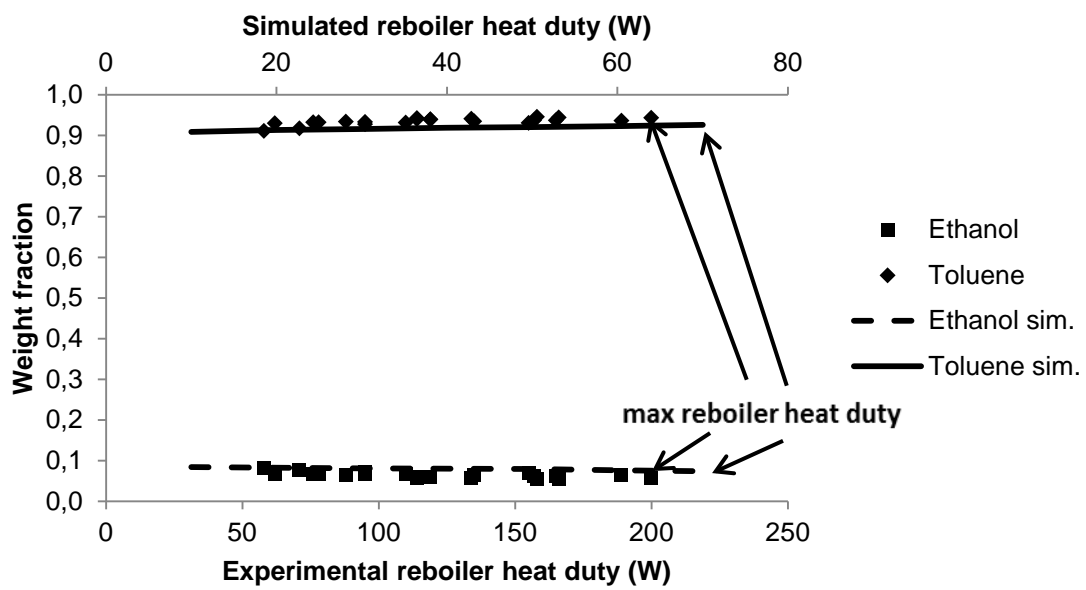
446  
 447 **Figure 4 c):** Mixture containing isooctane. Plot of several variables against reboiler heat duty:  
 448 Experimental and simulated composition (% w/w) of water in the bottoms product.  
 449

450



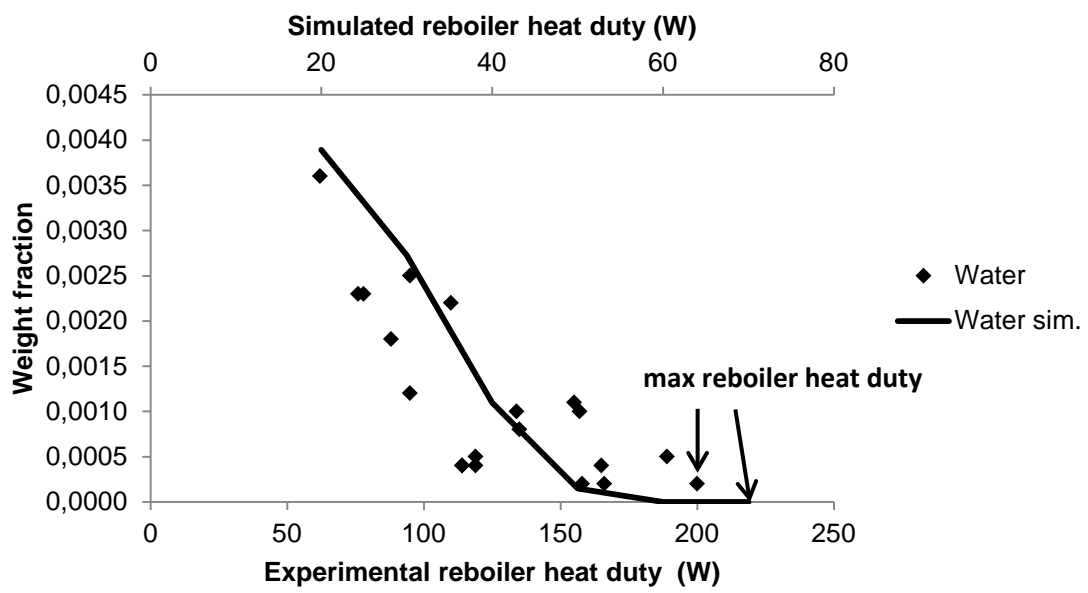
451  
452  
453  
454

**Figure 5 a):** Mixture containing toluene. Plot of several variables against reboiler heat duty: Experimental and simulated top and bottoms product flow rates

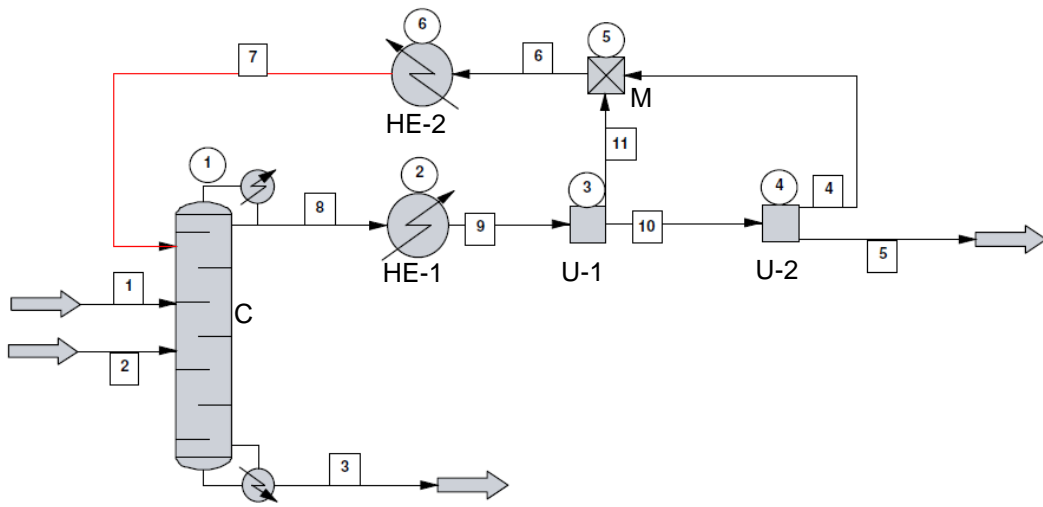


455  
 456 **Figure 5 b):** Mixture containing toluene. Plot of several variables against reboiler heat duty:  
 457 Experimental and simulated composition (% w/w) of ethanol and toluene in the column  
 458 bottoms  
 459





460  
 461 **Figure 5 c):** Mixture containing toluene. Plot of several variables against reboiler heat duty:  
 462 Experimental and simulated composition (% w/w) of water in the bottoms product.  
 463  
 464



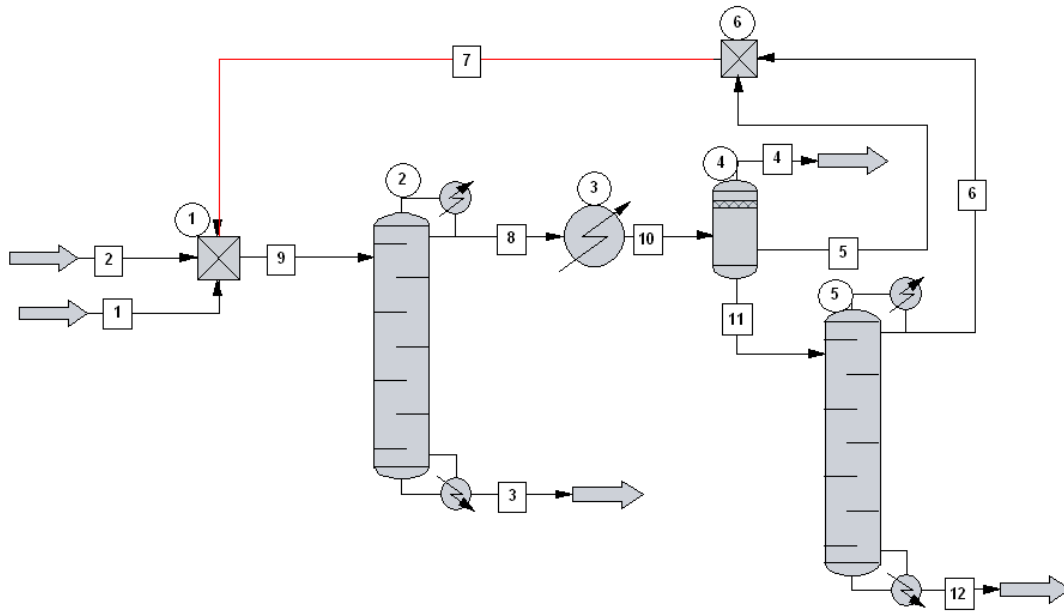
465

466

**Figure 6:** Schematic diagram for the Chemcad simulation.

467

468



469  
470  
471  
472  
473

**Figure 7:** Schematic diagram used to compare both processes.